Proceedings of the International Congress on Advances in Applied Physics and Materials Science, Antalya 2011

Monitoring of Heat Treatment Processes by High Energy Synchrotron Radiation

U. Klemradt[a], T. Rieger[b], K. Herrmann[b], D. Carmele[a], S. Meyer[a], T. Lippmann[c], A. Stark[c] and W. Bleck[b]

[a]II. Institute of Physics B, RWTH Aachen University, D-52064 Aachen, Germany

[b]Department of Ferrous Metallurgy, RWTH Aachen University, D-52064 Aachen, Germany

[c]Institute of Materials Research, Helmholtz-Zentrum Geesthacht, D-21502 Geesthacht, Germany

Advanced engineering materials are frequently based on multiphase microstructures, where the decisive step is the heat treatment adjusting the desired microstructure. A typical example are transformation-induced plasticity assisted steels, where the steel grades depend on the phase composition and the deformation-induced transformation of retained austenite into martensite. Usually methods for microstructural characterization are only applied after completion of the heat treatment process and comprise typically microscopy and X-ray analysis with laboratory tubes. Both methods can suffer from artefacts and probe a relatively small surface or volume, respectively. However, in the last decade synchrotron facilities have become available that offer very hard X-rays, which open up new possibilities for the observation of heat treatment processes owing to the unique combination of extremely high intensities with large penetration depths (mm scale). Sophisticated sample environments allow for complex *in situ* experiments, currently with a time resolution on the order of seconds. Only recently a commercial dilatometer of type Bähr Dil805AD has become available at the HARWI-2 beamline at the HASYLAB. This experimental setup was used for the *in situ* investigation of the quenching and partitioning process in transformation-induced plasticity steels. The experiments were performed in transmission at a wavelength of 0.0124 nm. The Debye–Scherrer rings were observed arising from statistical grain distributions characteristic for each microstructure. The time-resolved measurements allow conclusions about the phases present in the sample, their lattice parameters, texture and grain size.

PACS: 61.05.cp, 81.05.Bx, 81.30.Kf, 81.40.Ef

1. Introduction

The microstructural features are decisive for the mechanical properties of steel materials. Influencing factors are the phase fractions and the local chemical composition, for example. Possible constituents of multiphase steels are polygonal ferrite, bainitic ferrite, carbides, martensite, and retained austenite. The latter plays a distinct role for transformation-induced plasticity assisted (TRIP-assisted) advanced high strength steels (AHSS). During plastic deformation retained austenite may transform to martensite. The martensitic transformation is accompanied by an increase in volume which causes plastic deformation in the adjacent ferritic regions. The induced mobile dislocations and the hard martensitic particles lead to significant local strain hardening. On the macroscopic scale, an increased uniform elongation is observed at an elevated strength level, giving rise to the so-called TRIP effect. The development of steel materials is fostered by the automotive industry where the safety exigencies increase constantly. Simultaneously, the demand for reduced fuel and exhaust gas emissions, respectively, requires the reduction of the vehicle weight. Both demands are matched by high strength steels exhibiting good ductility. Recent innovations in steel materials are based on the advantageous combination of multiple phases. The first generation of AHSS extended the range of mechanical properties to very high strength levels at relatively low elongation values in martensitic steels to reduced strength levels at higher elongation values (TRIP steels), ferritic-martensitic dual phase (DP) steels and complex phase (CP) steels. The second generation used the stabilization of austenite by manganese alloying resulting in very high strength and elongation values. Current research activities aim to establish the third generation of AHSS providing medium strength and ductility levels at reduced production costs, aiming at an uncomplicated integration in existing process chains (Fig. 1).

In this context the so-called "quenching and partitioning" process was proposed in 2003 [1–5]. The "quenching and partitioning" (Q&P) concept defines a heat treatment procedure designed to stabilize retained austenite in a matrix of carbon-depleted martensite (Fig. 2). The latter is a substitute for the polygonal and the bainitic ferrite in conventional TRIP-assisted steels. The martensitic matrix is expected to increase the global strength level while retained austenite assures a satisfying ductility due to the TRIP effect. The heat treatment process involves partial or complete austenitization, which is followed by an interrupted quenching to quenching temperature QT, signifying the quench temperature between the martensite start temperature M_s and martensite finish temperature M_f. After this first quenching an

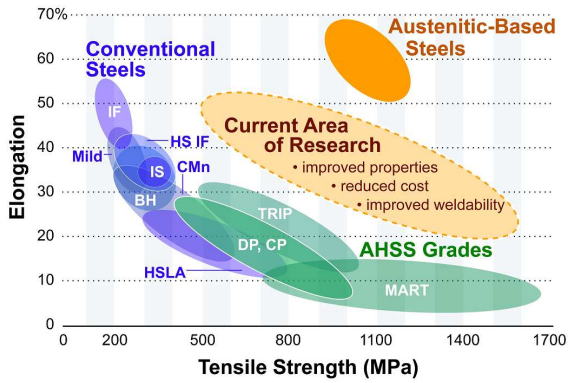

Fig. 1. Property range of established and emerging steel grades [1].

isothermal holding period follows at *QT* (1 step Q&P) or at an elevated partitioning temperature *PT* (2 step Q&P). During isothermal holding, a temperature- and time-dependent amount of carbon diffuses from the supersaturated martensite to austenite, hence reducing the M_f temperature below room temperature. Consequently, austenite remains stable during the concluding quenching to room temperature.

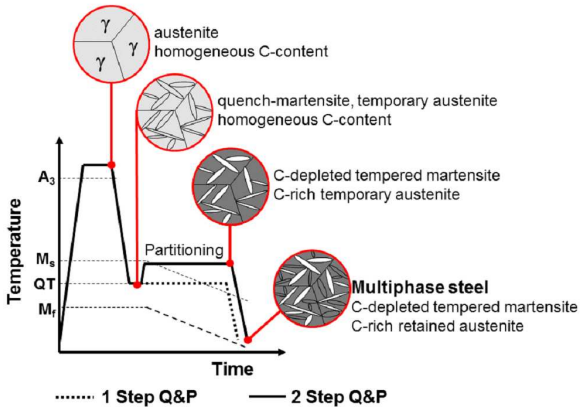

Fig. 2. Schematic microstructure evolution during "quenching and partitioning".

The heat treatment concept is accompanied by an adequate alloying concept typical for TRIP-assisted steel grades. Crucial are additions of aluminum or silicon because both elements are known to retard the formation of carbides. Carbides are undesired because their precipitation might occur during isothermal holding (partitioning) and hence consume carbon intended to chemically stabilize the retained austenite. Furthermore, the global carbon content is limited especially for automotive sheet steel in order not to deteriorate the weldability. Manganese acts as solid solution strengthener and reduces the critical cooling rate [2, 5–10].

The characterization of the resulting microstructure comprises in scientific and industrial practice optical and electron microscopy, dilatometry, diffraction methods and also magnetic measurements. Usually, microscopy and diffraction with laboratory X-ray tubes demand a prior metallographic preparation. Specimens are cut after completion of the heat treatment and embedded in polymers for grinding, polishing with abrasives and finishing by electrolytic polishing. For optical microscopy and SEM investigations, the contrast of the microstructure constituents is developed by selective etching or phase-sensitive deposition of chemical reactants on the specimen surface (color etching). Diffraction methods like electron backscatter diffraction (EBSD) and X-ray diffraction with laboratory tubes clearly distinguish the present phases by their crystallographic features. In AHSS austenitic parts (face centered cubic, fcc) are reliably separated from body centered cubic (bcc) microstructure constituents. It is noted that the latter may contain bainitic ferrite with high crystallographic imperfection and tetragonally distorted martensite. For transmission electron microscopy (TEM) thin foils on the submicron scale are prepared in intense and delicate preparation procedures. Magnetic methods distinguish the nonmagnetic austenitic volume fractions from the remaining magnetic constituents, i.e. polygonal and ferritic ferrite and martensite [11–14].

Still, the established methods suffer from severe disadvantages. Phases with similar chemical potential (like bainite, martensite and retained austenite) are hard to distinguish by color etchants for optical microscopy or for SEM. Also both methods are limited in their resolution and the phases are often identified based on the experience of the investigator instead of objective and precise criteria. Frequently, the phase fractions are only estimated. Except for the magnetic measurements, all mentioned methods investigate the surface or near-surface region of the specimens, which remains relatively small. Furthermore the preceding sample preparation may especially affect metastable microstructure constituents like retained austenite. Only the magnetic measurements are applicable to bulk specimens without prior preparation. Moreover, none of the methods is used at elevated temperatures, direct evidence on the microstructure evolution during the processing is hence lacking so far [14, 15]. In the present work the *in situ* characterization of heat treatment processes by diffraction experiments with high-energy synchrotron radiation is discussed.

2. Experimental approach

Firstly, the usefulness of high energy synchrotron radiation (100 keV) for steel diffraction is illustrated by comparison to diffraction experiments with Co K_α (6.9 keV) radiation produced by a laboratory tube. Secondly, the method is applied to monitor the evolution of the austenite phase fraction during Q&P.

Two diffractograms of the standardized automotive TRIP-steel HCT690T [16] were obtained from diffraction of Co K_α and synchrotron radiation and compared to

each other. For the *in situ* experiments with synchrotron radiation the Si/Ni alloyed TRIP steel QPSN was investigated. While the contents of carbon, silicon and manganese correspond to industrialized TRIP-assisted steels, the alloy QPSN was enriched with nickel to further decrease the critical cooling rate.

TABLE

Chemical composition of investigated steels [mass%], (n.a. — not analyzed).

Alloy	C	Si	Mn	P	S	Al	N	Ni
HCT690T	0.248	0.036	1.623	< 0.120	< 0.015	1.246	n.a.	0.01
QPSN	0.200	1.910	1.640	< 0.002	< 0.010	n.a.	0.002	3.10

The chemical compositions of the investigated steels are given in Table. The alloy QPSN was melted in a laboratory vacuum furnace and cast to ingots of 140 mm × 140 mm × *ca.* 500 mm. To destroy the as-cast microstructure, the ingots were cut inTO two pieces of around 250 mm, reheated to 1200 °C and deformed to a cross--section of 70 mm × 70 mm. After normalization (austenitization at 970 °C for 60 min., air cooling), specimens of 7 mm×4 mm×1.3 mm were machined from bulk material at a distance of 6.5 mm from the surface. For the laboratory diffraction experiments the specimens were moulded in cold hardening resin and metallographically prepared. The preparation procedure consisted of grinding (SiC abrasives), polishing with diamond particles (6 μm/3 μm) in aqueous dispersion and finishing in an electrolytical polishing machine. Conventional diffraction experiments in reflection geometry were performed with Co K_α radiation using a collimator (0.3 mm) and a total integration time of 2000 s. By contrast, diffraction experiments in transmission geometry were performed at the high energy materials science beamline HARWI-II operated by the Helmholtz–Zentrum Geesthacht at HASYLAB, DESY. The monochromator was tuned to a photon energy of 100 keV corresponding to a wavelength of 0.124 Å. The Debye–Scherrer rings were recorded during an exposure time of 1 s with a flat panel detector of type MAR555. Powder diffractograms were obtained by azimuthal integration and evaluated by a Rietveld refinement using the commercial software TOPAS in the academic version 4.0. From the refined pattern the phase fraction of austenite and the austenite lattice parameter were extracted to monitor the phase transformation and the carbon content, which is related to the austenite lattice parameter. The heat treatment was effectuated in a state-of-the-art dilatometer (Bähr Thermoanalyse 805AD) modified for *in situ* measurements at a synchrotron beamline. Inductive heating with 25 K/s and Ar gas cooling with a controlled $t_{8/5}$-time of 17 s were applied. Results are presented for 2 step Q&P of the alloy QPSN with a quench temperature QT = 280 °C and a partitioning time of 70 s at the partitioning temperature PT = 450 °C.

3. Results and discussion

A relative advantage of the usual X-ray tube based characterization of steel is the resulting penetration depth on the micron scale. For comparison, electron backscatter diffraction typically probes only some ten nanometers underneath the surface. In Fig. 3a the penetration depth of X-rays in iron is shown as a function of the photon energy. The dip at 7.2 keV is caused by the *K*--absorption edge of iron, reducing the penetration depth from more than 20 to less than 5 μm. Single-wavelength diffraction experiments with laboratory X-ray tubes employ the characteristic radiation emitted by the target material, typically copper, cobalt or molybdenum. With photon energies (K_α-lines) of 8.0 keV, 6.9 keV and 17.4 keV, respectively, the penetration depths remain on the micron scale [17].

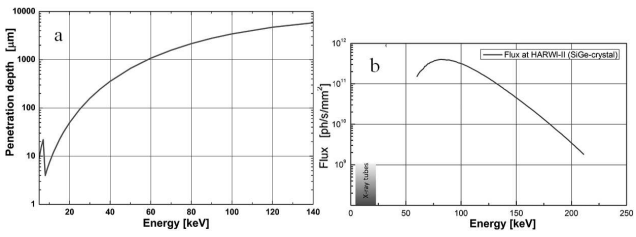

Fig. 3. Penetration depth in iron as function of the photon energy (a) and photon flux at the HARWI-II beamline (b). For comparison, the shaded area indicates roughly the operation range of typical laboratory X-ray tubes.

By contrast, at a synchrotron the photon energy is not restricted to certain values, and much higher energies are available at excellent flux. It should be noted that already for 60 keV photons the penetration depth reaches the millimeter scale. Consequently, macroscopic volumes of sheet steel can be probed [18]. At the HARWI-II beamline used here, photon energies between 60 and 240 keV are available with a (monochromatic) photon flux several orders of magnitude higher than that of laboratory tubes (cf. Fig. 3b). As a result, the exposure time can be reduced to seconds compared to hours necessary with X-ray tubes.

In Fig. 4 two diffractograms of the automotive TRIP--steel HCT690T are displayed, which were obtained by diffraction experiments with synchrotron radiation at 100 keV and by Co K_α radiation. Though the angular

range is necessarily much smaller for the high energy radiation, the large number of detected peaks is obvious, resulting from the much larger part of reciprocal space accessible with 100 keV radiation [18]. Additionally, the peaks are more distinct, for example the $\{220\}_{\mathrm{fcc}}$ peak is clearly separated using synchrotron radiation but hardly distinguishable from the background using Co radiation. Hence a better quantitative analysis of the diffraction pattern can be expected from synchrotron experiments.

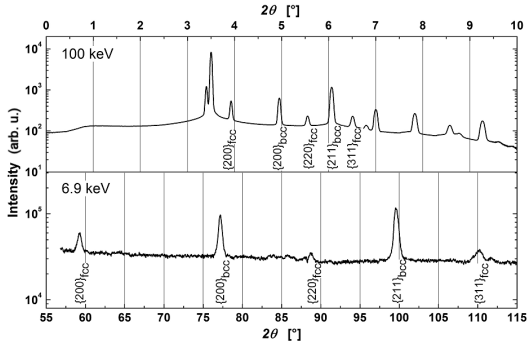

Fig. 4. Diffractograms of TRIP steel HCT690T obtained by diffraction experiments with synchrotron (100 keV) and Co K_a (6.9 keV) radiation.

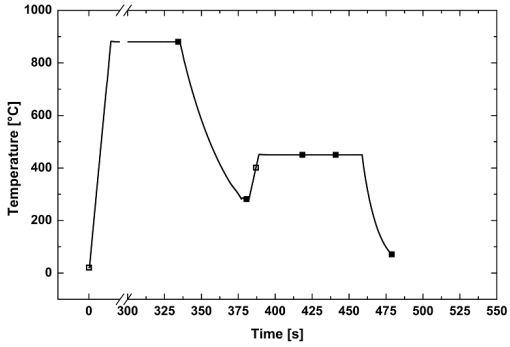

Fig. 5. Measured time–temperature cycle of 2 step Q&P (steel QPSN). Symbols indicate diffraction experiments.

The microstructure evolution was investigated *in situ* during 2 step Q&P processing of the alloy QPSN. Figure 5 shows the time–temperature cycle with diffraction experiments indicated as points, with open and full symbols referring to different runs. It should be mentioned that the time interval between two successive exposures was limited in practice by technical aspects of the detector.

In Fig. 6, exemplary 2D diffraction patterns are shown which were recorded at the austenizing temperature AT

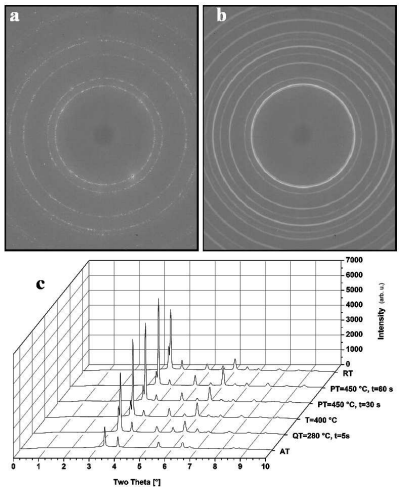

Fig. 6. Recorded diffraction patterns at the austenizing temperature AT (a) and after Q&P processing at room temperature (b), diffractograms at various process steps obtained by azimuthal integration (c).

and at room temperature RT after Q&P processing. For quantitative analysis, the diffraction patterns were azimuthally integrated resulting in powder diffractograms (Fig. 6c). The data already allow us a qualitative evaluation of the experiments. Evidently, the intensity pattern is of the Debye–Scherrer type, although the rings are not completely occupied at AT. This is because individual grains are subject to coarsening during holding at the elevated temperature of 950 °C, resulting in texture. The latter may be used to characterize (and ultimately optimize) the austenizing process especially for cold rolled steel strip, which is heat-treated to properly adjust the desired microstructure. For homogeneous properties the rolling texture should be significantly reduced which can be validated by the occupation of the Debye–Scherrer rings. In the course of the heat treatment the change of the peak positions and intensities is obvious for both the Debye–Scherrer rings and the integrated diffractograms. The decisive steps of the microstructural evolution are hence visible at a glance and are easily identified as a starting point for further investigations.

Quantitative results obtained by the Rietveld refinement are displayed in Fig. 7. The austenite fraction decreases significantly during continuous cooling from AT to QT and further during cooling from PT to RT owing to phase transformations. Additionally, an isothermal phase transformation seems to take place at PT. The reheating from QT to PT has a negligible effect on the austenite fraction compared to the isothermal decrease in the first 30 s at PT. Between 30 and 60 s at PT, only a marginal change in the austenite fraction is measured. At room temperature more than 15% retained austenite are stabilized. As expected, the austenite lattice parameter changes during the Q&P process, illustrated by the severe jump from *ca.* 3.615 Å at 400 °C to around 3.630 Å

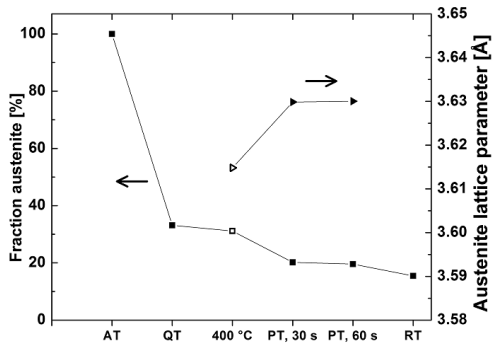

Fig. 7. Austenite fraction and lattice parameter during Q&P processing (AT = 950°C/300 s, QT = 280°C/5 s, PT = 450°C/70 s). Open and full data points refer to different runs.

at 450°C. This is an indicator for the austenite carbon content: the larger the lattice parameter, the higher the carbon content. The two measured values of the austenite lattice parameter at the partitioning temperature do not change significantly. This suggests that no (further) carbon enrichment of austenite occurs after 30 s for the given Q&P conditions.

4. Conclusions

In summary, the promising "quenching and partitioning" heat treatment results in a complex microstructure with martensitic and austenitic constituents on a submicron scale. The use of hard synchrotron X-ray radiation provides an ideal instrument for the investigation of the microstructure evolution during the heat treatment process. Photon energies above 60 keV allow us the penetration of steel sheets on the mm scale without prior preparation and the investigation of macroscopic, representative sample volumes. The combination of a short X-ray wavelength with a flat panel detector provides access to a large part of reciprocal space in one experiment. As a result also highly indexed peaks are detected and contribute to the quantitative analysis of the phase constituents. Due to the high photon flux the exposure time is reduced to one second, allowing for an *in situ* monitoring of the microstructure development during the heat treatment process.

The method was successfully applied for the investigation of a Si-/Ni-alloyed TRIP steel. An austenite transformation during continuous cooling and isothermal partitioning was observed and quantified. The nearly constant austenite lattice parameter indicates that no further carbon enrichment took place after 30 s at PT for the investigated Q&P conditions.

As a next step, the experiments will be extended to the mechanical properties of the resulting microstructures. In the future it will be interesting to follow Q&P processes with improved time resolution, since sub-second exposure times are expected for the next detector generation.

Acknowledgments

The authors gratefully acknowledge funding by Exploratory Research Space (ERS) at RWTH Aachen University (OPPa110) and especially the support in TOPAS Academic by Dr. Lars Peters.

References

[1] International Iron & Steel Institute — Committee on Automotive Applications, Advanced High Strength Steel (AHSS) Application Guidelines, version 4.1, `www.worldautosteel.org`, (06/2009), last accessed 25.03.2011.

[2] D.V. Edmonds, D.K. Matlock, J. Speer, in: *Proc. Int. Conf. Advanced Steels 2010*, Eds. Y. Weng, H. Dong, Y. Gan, Metallurgical Industry Press, Beijing 2010, p. 229.

[3] H. Hofmann, D. Mattissen, T.W. Schaumann, *Mat.-wiss. Werkstofftech.* **37**, 716 (2006).

[4] D.K. Matlock, J. Speer, in: *Microstructure and Texture in Steels and Other Materials*, Ed. A. Haldar, S. Suwas, D. Bhattacharjee, Springer, London 2009, p. 185.

[5] J. Speer, D.K. Matlock, B.C. DeCooman, J.G. Schroth, *Acta Mater.* **51**, 2611 (2003).

[6] D.V. Edmonds, K. He, F.C. Rizzo, B.C. De Cooman, D.K. Matlock, J. Speer, *Mater. Sci. Eng. A* **438-440**, 25 (2006).

[7] D.V. Edmonds, K. He, M.K. Miller, F.C. Rizzo, A. Clarke, D.K. Matlock, J. Speer, *Mater. Sci. Forum* **539-543**, 4819 (2007).

[8] P. Jacques, E. Girault, T. Catlin, N. Geerlofs, T. Kop, T.S. van der Zwaag, F. Delannay, *Mater. Sci. Eng. A* **273-275**, 475 (1999).

[9] J. Speer, D.K Matlock, *J. Jpn. Soc. Heat Treatment* **49**, 415 (2009); special Issue on the *17th IFHTSE Congress, Kobe*, 2008.

[10] C.Y. Wang, J. Shi, W.Q. Cao, H. Dong, *Mater. Sci. Eng. A* **527**, 3442 (2010).

[11] J. Angeli, E. Fuereder, M. Panholzer, A.C. Kneissl, *Prakt. Metallogr.* **43**, 489 (2006).

[12] E. Fuereder, C. Voit, J. Pühringer, M. Pohl, *Prakt. Metallogr.* **47**, 375 (2010).

[13] S. Melzer, J. Moermann, in Ref. [4], p. 267.

[14] L. Zhao, N.H. van Dick, E. Brueck, J. Sietsma, S. van der Zwaag, *Mater. Sci. Eng. A* **313**, 145 (2001).

[15] M.J. Santofimia, L. Zhao, R. Petrov, J. Sietsma, *Mater. Char.* **59**, 1758 (2008).

[16] Draft European Standard prEN 10338:2010, *Hot rolled and cold rolled non-coated products of multiphase steels for cold forming — Technical delivery conditions.*

[17] J.A. Bearden, *Rev. Mod. Phys.* **39**, 78 (1967).

[18] K.-D. Liss, A. Bartels, A. Schreyer, H. Clemens, *Textures Microstruct.* **35**, 219 (2003).